

# Radiation Processes in GRBs. Prompt Emission

Mikhail V. Medvedev

*Department of Physics and Astronomy, University of Kansas, Lawrence, KS 66045*

**Abstract.** A substantial fraction of prompt GRB spectra have soft spectral indexes exceeding the maximum allowed by the synchrotron model  $\alpha_{max} = -2/3$ . Some spectra also exhibit very sharp break at  $E_p$ , inconsistent with the smooth synchrotron spectra. These facts pose a serious problem for the “optically thin synchrotron” interpretation of the prompt emission. We review various models suggested in order to resolve this puzzle.

## INTRODUCTION

Time-resolved spectral analyzes of *BATSE* and *BeppoSAX* [1, 2] clearly demonstrate that 30-50% of spectra violate the so-called “synchrotron line of death” (LoD), i.e., they have the soft photon indexes  $\alpha$  greater than  $-2/3$  (note,  $F_\nu \propto \nu^{\alpha+1}$ ). In addition, a significant number of the spectra are better fit with the sharply broken power-law (BPL) model than with the smooth Band function. These facts make the simplest synchrotron interpretation of the prompt GRB emission at least questionable. Some attention has been paid to this problem and here we review alternative models suggested by several authors.

## SELF-ABSORBED SYNCHROTRON MODEL

The simplest model which can produce a hard spectrum at low energies suggests that synchrotron radiation may be self-absorbed. This possibility has been considered by several authors; for more discussion and references, see Ref. [3]. The low-energy power-law index depends on the relative values of the self-absorption frequency  $\nu_a$  and the peak synchrotron frequency  $\nu_m$ :

$$F_\nu \propto \begin{cases} \nu^{5/2}, & \text{for } \nu_m < \nu \ll \nu_a; \\ \nu^{1/3}, & \text{for } \nu_a < \nu < \nu_m; \\ \nu^2, & \text{for } \nu \ll \min(\nu_m, \nu_a). \end{cases} \quad (1)$$

Note that the second case corresponds to the optically thin regime. A typical self-absorbed spectrum with  $\nu_m < \nu_a$  is shown in Fig. 1(a) by the curve labeled SAS. In addition to a large spectral index, a self-absorbed spectrum has also a much narrower peak than the optically thin spectrum. Both these properties often lead to improved spectral fits of LoD-violating and BPL bursts.

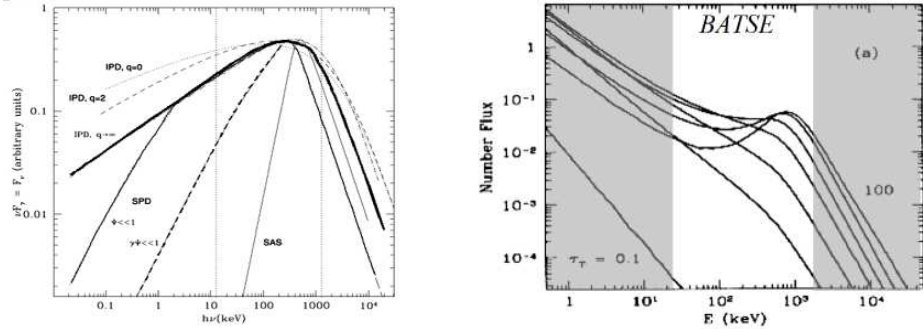


**FIGURE 1.** (a) The synchrotron self-absorbed spectrum (SAS) and the synchrotron spectrum in the small pitch-angle regime (from [3]), the thick solid line shows a standard synchrotron spectrum for comparison. (b) The spectrum produced by saturated Comptonization (from[4]).

What conditions of a fireball are needed to have the self-absorption frequency in the *BATSE*'s spectral window? The optical depth to synchrotron self-absorption

$$\tau \sim \left( \frac{l}{10^{13} \text{ cm}} \right) \left( \frac{n}{10^8 \text{ cm}^{-3}} \right) \left( \frac{B}{10^8 \text{ G}} \right)^{2/3} \left( \frac{\gamma_m}{50} \right)^{-8/3} \left( \frac{\Gamma}{10^3} \right)^3 \left( \frac{\nu_{obs}}{10^{19} \text{ Hz}} \right)^{-5/3} \quad (2)$$

must be of order unity for the observed frequency  $\nu_{obs}$  to be in the *BATSE* range. Here  $l$  and  $n$  are the line-of-sight path length and particle density in the co-moving frame,  $\gamma_m$  and  $\Gamma$  are the minimum Lorentz factor of power-law electrons and the bulk Lorentz factor of the ejecta, and  $B$  is the co-moving magnetic field strength. Apparently, the values of the parameters are rather extreme, e.g., the magnetic field strength is (much) greater than the equipartition field of  $\sim 10^5 \dots 10^6$  G, typically assumed within the standard synchrotron shock model (SSM). Another problem of this model is a very low efficiency of the fireball shock because the peak synchrotron frequency (where most of the energy is emitted) is deeply in the optically thick range.

## SATURATED COMPTONIZATION MODEL

Another model that may be of interest to us is the so-called *saturated synchrotron self-Compton* proposed in a series of papers (see e.g., Ref. [4]) primarily in an attempt to explain the spectral peak energy – fluence anti-correlation observed in several long, bright, smooth GRBs. The model proposes that impulsively accelerated, non-thermal, relativistic electrons (and, perhaps, pairs) repeatedly Compton up-scatter self-emitted radio/infrared synchrotron photons into gamma-ray energies. The Thompson optical depth is initially large,  $\tau_T \gg 1$ , so that the emerging gamma-rays are in thermal equilibrium with electrons and  $\alpha$  approaches the Wien limit,  $\alpha = +2$ , whereas the synchrotron soft-photon source is strongly self-absorbed by internal free-free and synchrotron opacities. As time goes on, the Thompson opacity decreases and for  $\tau_T \ll 1$  the spectrum reduces to a single-scattering Compton spectrum with the slope  $\alpha = -(p+1)/2$  (for the electron distribution  $N(E) \propto E^{-p}$ ). Thus, this model can naturally explain the hard-to-soft evolution in prompt GRB spectra.

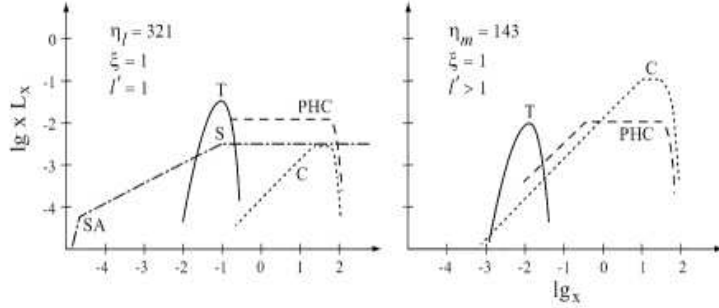


**FIGURE 2.** Spectra predicted by the photospheric model (from [5]).

Typical spectra are shown in Fig. 1(b) for various values of  $\tau_T$ . It is quite clear that the emerging spectrum differ dramatically from the Band spectrum (even within a narrow BATSE window) which nicely fits the majority of GRBs. The required values of the fireball parameters are also not very likely: the comptonizing electrons ought to be “warm” with  $\gamma_e \sim$  few (in contrast to the SSM, in which electrons are in near equipartition, hence  $\gamma_e \sim 1000$ ) and the required magnetic fields are also too weak,  $B \sim 0.1 \dots 10$  G.

## PHOTOSPHERIC MODEL

A synthetic model incorporating a standard synchrotron internal shock model and an extended photosphere can also explain steep low-energy spectra [5]. In this model synchrotron photons are re-processed in the photosphere. The single-scattering Comptonized and photospheric components naturally have low-energy spectra with  $\alpha = 0$ . Fig. 2 shows some examples; here T: thermal photosphere, PHC: photospheric comptonized component, S: shock synchrotron, C: shock pair-dominated comptonized component. For a detailed discussion the reader is referred to Ref. [5]. The weakness of this model is that it requires moderate Thompson opacities  $\tau_T \sim 1$  which, in turn, requires either fine tuning of plasma parameters or, alternatively, some sort of self-regulated pair opacity which produces the column density which self-adjusts itself to a column density of few  $\text{g cm}^{-2}$ . This model also requires very low baryonic load, that is, large bulk Lorentz factors  $\Gamma > 1000$ .

## SMALL PITCH-ANGLE RADIATION MODEL

Optically thin synchrotron radiation has a low-energy asymptotic power-law index  $\alpha = -2/3$  only if the the emitting electrons have an isotropic distribution. For electrons having anisotropic velocity distribution this may not be the case. Let us consider a beam of mono-energetic highly-relativistic electrons ( $\gamma_e \gg 1$  is their Lorentz factor) propagating almost along a homogeneous magnetic field, so that the parallel velocity is

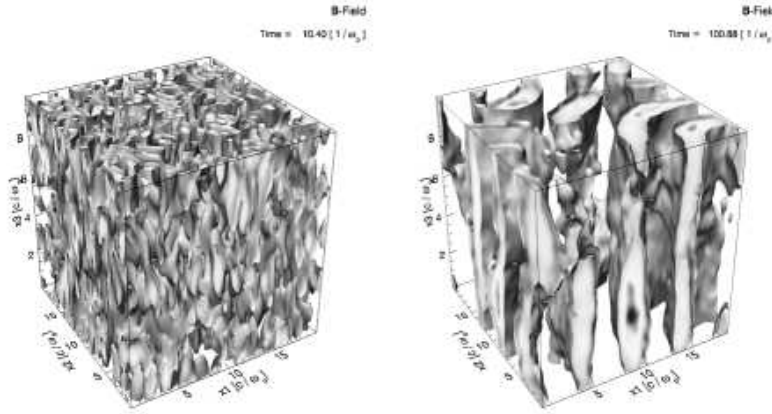


**FIGURE 3.** The magnetic field 3D structure (surfaces of constant  $B^2$ ) at a relativistic shock (from [7]).

much larger than the transverse velocity:

$$v_{\perp}/v_{\parallel} \sim \Psi \ll 1/\gamma_e, \quad (3)$$

where  $\Psi$  is the pitch-angle. In this case, from  $v^2 = v_{\parallel}^2 + v_{\perp}^2$  and  $1 - v^2 = 1/\gamma_e^2$  it follows that the transverse motion of such electrons is non-relativistic,  $v_{\perp} \ll 1$ . Radiation emitted by these electrons will be *cyclotron* (not synchrotron), relativistically boosted with the Lorentz factor  $\sim \gamma_e$  along the magnetic field. The low-energy asymptotic spectrum of cyclotron radiation is steeper,  $\alpha = 0$ . This is called the “small pitch-angle” regime.

Small pitch-angle radiation has been suggested as yet another way of producing steep low-energy spectra, see Ref. [3] and references therein. The typical spectra for  $1/\gamma_e < \Psi \ll 1$  and  $\Psi \ll 1/\gamma_e$  are shown in Fig. 1(a) by the curves labeled SPD. Note that in the latter case, the spectrum has a very sharp break. Thus, this model can naturally explain both LoD-violating and BPL bursts. The small pitch-angle radiation model relies, however, on a crucial assumption: a highly anisotropic electron distribution is somehow created and maintained at the shock. Moreover, it is a well-known fact that (highly) anisotropic particle distributions are always unstable with respect to a number of plasma instabilities. Finally, in the small pitch-angle regime only the transverse energy  $\sim m_e v_{\perp}^2/2$  can be converted into radiation. Because of the condition  $v_{\perp}/v_{\parallel} \ll 1/\gamma_e$  with  $\gamma_e \sim 1000$  or more, the radiation efficiency will be enormously low.

## JITTER RADIATION MODEL

It is now becoming a widely accepted fact that magnetic fields of sub-equipartition strength are generated at the front of a relativistic shock via the two-stream (or Weibel) instability. The magnetic field generation has been predicted theoretically [6] and then confirmed via 3D PIC kinetic simulations [7, 8]. The produced magnetic fields have rather unusual properties. The field is predominantly generated in the direction, perpendicular to the shock propagation direction. In the plane of the shock, the field is highly

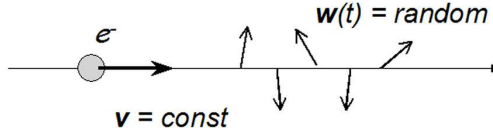


**FIGURE 4.** An electron motion in the jitter regime.

chaotic with the correlation length being of order the relativistic skin depth

$$\lambda_s \simeq \frac{c\sqrt{\gamma_s}}{\omega_{ps}} \sim (3 \text{ cm}) \gamma_e^{1/2} \left( \frac{m_s}{m_e} \right)^{1/2} \left( \frac{n_s}{10^{10} \text{ cm}^{-3}} \right)^{-1}, \quad (4)$$

where  $\omega_{ps} = (4\pi e^2 n_s / m_s)^{1/2}$  is the non-relativistic co-moving plasma frequency of species  $s = e^-, p$  (both species, electrons and protons, generate the field). A typical strength of the field is  $\epsilon_B = B^2 / (8\pi \Gamma n m_p c^2) \sim 10^{-3}$  (here  $n$  is the density downstream). The correlation scale  $\lambda$  is not constant, rather it increases with time, i.e., with the distance from the shock front. Fig. 3 represents three-dimensional contours of constant  $B^2$  close to the shock front and far downstream.

It can straightforwardly be evaluated that the correlation length of the electron-produced field,  $\lambda_e$ , is much smaller than the Larmor radius of a relativistic radiating electron,  $\rho_e$ . The electron trajectory is not helical, so the standard synchrotron theory is not applicable. Quantitatively, jitter regime (for details, see Ref. [9]) occurs when the deflection angle of the electron is smaller than the relativistic beaming angle  $\sim 1/\gamma_e$ , i.e.:

$$\delta \sim \lambda_e / (\rho_e / \gamma_e) \sim (eB\lambda_e) / (m_e c^2) < 1. \quad (5)$$

In the case  $\delta \ll 1$ , the particle motion may safely be approximated as straight. As the electron moves at a constant velocity, it experiences short accelerations in random directions, perpendicular to the direction of motion, as represented in Fig. 4. The power spectrum of radiation is obtained from the Lienard-Wichert potentials:

$$\frac{dW}{d\omega} = \frac{e^2 \omega}{2\pi c^3} \int_{\omega/2\gamma_e^2}^{\infty} \frac{|\mathbf{w}_{\omega'}|^2}{\omega'^2} \left( 1 - \frac{\omega}{\omega' \gamma_e^2} + \frac{\omega^2}{2\omega'^2 \gamma_e^4} \right) d\omega', \quad (6)$$

where  $\mathbf{w}_{\omega'} = \int \mathbf{w} e^{i\omega' t} dt$  is the Fourier component of the particle's acceleration, which is related to the spectrum of the magnetic field as  $w_{\omega'} = (eB_{\omega'}) / (\gamma_e m_e) = (eB_{k'}) / (\gamma_e m_e c)$ . For a standard energy distribution of electrons (power-law with a cutoff at low energies,  $\gamma_{e,min}$ ), the resultant spectrum is shown in Fig. 5(a). It is well described by a BPL model with  $\alpha = 0$ , the high energy exponent  $\beta = -(p+1)/2$ , and the jitter break frequency:

$$\nu_j \simeq (c/\lambda_e) \gamma_{e,min}^2 \Gamma \sim (10^{10} \text{ Hz}) \gamma_{e,min}^{3/2} \Gamma. \quad (7)$$

Note that this frequency is independent of the magnetic field strength.

Unlike the electron-produced fields, the proton-produced magnetic field has a larger spatial correlation scale,  $\lambda_p$ , for which  $\delta > 1$ . An electron radiates synchrotron radiation

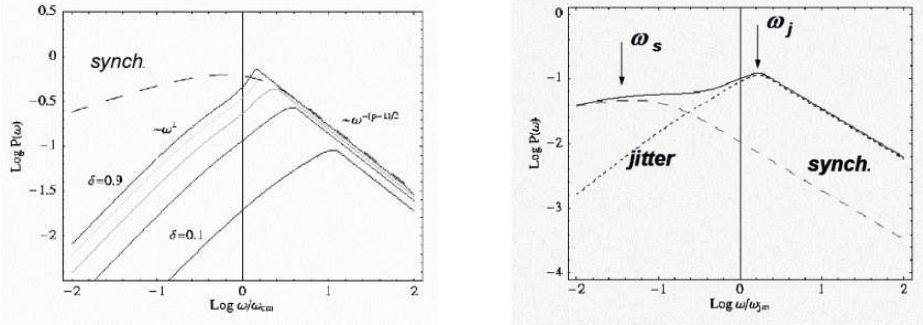


**FIGURE 5.** (a) The spectrum of jitter radiation for the power-law distributed electrons (from [9]). (b) A generalized jitter+synchrotron spectral model (from [9]).

in such a field. Also, a large-scale magnetic field may be ejected from a magnetized progenitor. Therefore, in general, the spectrum may consist of two components, a jitter component (due to small-scale fields,  $B_{SS}$ , with  $\delta < 1$ ) and a synchrotron component (due to large-scale fields,  $B_{LS}$ , with  $\delta > 1$ ), as in Fig. 5(b). The jitter-to-synchrotron peak frequency ratio and the ratio of the *photon* fluxes at these peak frequencies uniquely determine two free parameters,  $\delta$  and  $B_{LS}/B_{SS}$ :

$$\frac{v_j}{v_m} \simeq \frac{3}{2} \frac{B_{LS}}{B_{SS}} \delta, \quad \frac{F(v_j)}{F(v_m)} \simeq \delta^2, \quad (8)$$

which offers a unique diagnostic of GRB shocks.

## CONCLUSIONS

We reviewed several models which has been proposed in order to resolve the puzzle of LoD-violating and BPL gamma-ray bursts. It seems that the jitter model is the most promising one, because it readily follows from the collisionless shock physics and results in minimal changes in the standard optically thin synchrotron shock model.

## REFERENCES

1. Preece, R. B., *et al.*, 2000, ApJS, 126, 19
2. Frontera, *et al.*, 2000, ApJS, 127, 59
3. Lloyd-Ronning, N. M. and Petrosian, V. 2002, ApJ, 565, 182
4. Liang, E., Kukunose, M., Smith, I. A., and Crider, A. 1997, ApJL, 479, L35
5. Mészáros, P. and M. J. Rees, ApJ, 530, 292
6. Medvedev, M. V., and Loeb, A. 1999, ApJ, 526, 697
7. Silva, L. O., Fonseca, R. A., Tonge, J. W., Dawson, J. M., Mori, W. B., and Medvedev, M. V. 2003, ApJL, 596, L121
8. Frederiksen, J. T., Hederal, C. D., Haugbølle, T., Nordlund, Å. 2003, astro-ph/0308104
9. M.V. Medvedev, M. V. 2000, ApJ, 540, 704